Orthotics and Prosthetics, Vol. 29, No. 3, pp. 25–27, September 1975

MATERIALS INVESTIGATION OF FAILED PLASTIC ANKLE-FOOT ORTHOSES

E. P. Lautenschlager[1], S. C. Bayne[1], R. Wildes[1], J. C. Russ[2], and M. J. Yanke[2]

In April 1974 the Department of Biological Materials received for analysis the Ortholen ankle-foot orthosis (AFO) that had failed as shown in Figure 1. This device was one of two worn bilaterally by an active man who weighed 175 lb., and was 5 ft. 11 in. tall. The failure began as a small crack at the base of the right angle, and then propagated slowly for several months until the integrity of the device became questionable.

The purpose of the investigation reported here was to determine the reason for failure and to make suggestions for the improvement of the orthosis.

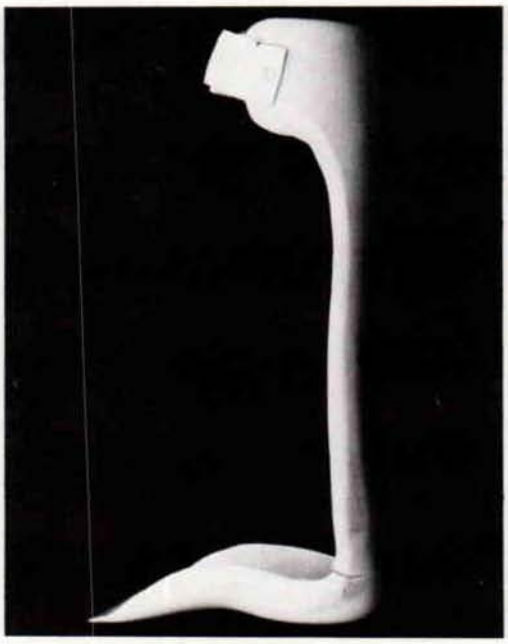

Fig. 1. Failed ankle-foot orthosis.

[1]Department of Biological Materials, Northwestern University, 311 East Chicago Avenue, Chicago, Ill. 60611.

[2]Prosthetic-Orthotic Center, Northwestern University, 345 East Superior Street, Chicago, Ill. 60611.

METHODS OF INVESTIGATION

After gross observations as to the influence of loading the device were made (Fig. 2), the orthosis was sectioned in the area of the failure, and scanning-electron micrographs (SEM) were taken of the fractured surface (Figs. 3 and 4).

In addition, four specimens for mechanical testing were cut from the device and tested in three-point bending in an Instron machine at a strain rate of approximately 0.4 per minute.

RESULTS

Figure 2 shows that downward loading near the ball of the foot places the right-angled area in a state of tension and opens up the crack.

Because tension opened the crack and the propagation was reported to be slow, fatigue was suspected as the mode of failure. Fatigue can occur with cyclic loads which are well below the ultimate or maximum load-bearing characteristics of the material. Because fatigue progresses in a stepwise fashion with a crack that is opened up a small additional amount during every cycle, it can be detected from a fracture surface characterized by small steps or striations. This is the case as shown in Figure 4 for the SEM of the fracture surface of the AFO supplied.

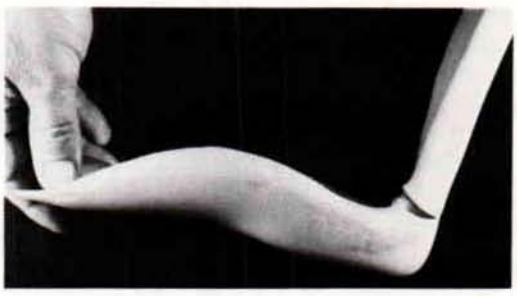

Fig. 2. Tensile loading opens up crack.

Fig. 3. Low magnification SEM of fracture surface. Area in white square presented in Figure 4.

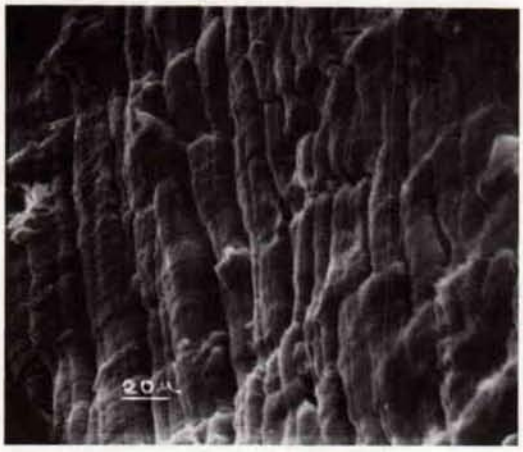

Fig. 4. High magnification SEM of fracture surface. Note the fatigue striations.

The bending strength, elastic modulus, and testing strain rate are listed in Table I as the average ± one standard deviation, as measured for four specimens. The formulae used in the calculations are as follows:

$$\text{Bending strength} = \frac{3}{2}\frac{PL}{BH^2}$$

$$\text{Modulus} = \frac{\Delta P L^3}{4BH^3\Delta y}$$

$$\text{Strain rate} = \frac{6H}{L^2}\cdot CS$$

where:

L = length between base support = 0.61 in.

P = yielding load applied at L/2,

B = breadth or width of specimen,

H = height or thickness of specimen,

$\Delta P/\Delta y$ = change of load per change of deflection in straight line elastic region of curves as shown in Figure 5,

CS = crosshead speed = 0.1 in./min.

When compared to other orthotic materials listed in Table 2, the strength of the material is among the weaker normally employed.

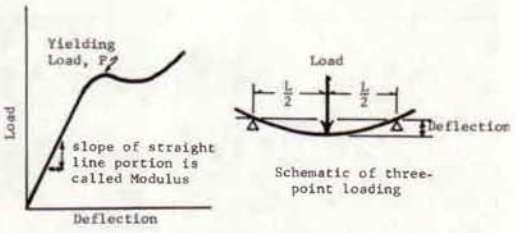

Fig. 5. Typical deformation curve obtained in three-point bending.

TABLE I. MECHANICAL PROPERTIES OF SPECIMENS SECTIONED FROM AFO SUPPLIED

Specimen	Thickness	Width	Bending Strength (psi)	Elastic Modulus (psi)	Strain Rate min^{-1}
1	.255	.499	7760	31970	0.41
2	.254	.490	7670	28640	.41
3	.257	.488	7390	24320	.41
4	.263	.485	6660	25920	.42
Avg ±s			7370±500	27710±3350	

TABLE 2. TYPICAL MECHANICAL PROPERTIES OF ORTHOTIC LAMINATES

Code Number	4110/Polylite Ratio**	Laminates*	Bending Strength (psi)	Modulus (psi)	Strain Rate min^{-1}
1A	50:50	GT/N/D	13,826±544	202,247±11086	.20±.01
1B	50:50	GL/N/D	14,223±628	243,280±33124	.20±.01
1C	70:30	GL/N/D	12,181±581	122,031±25298	.27±.01
1D	70:30	N	6,539±495	154,085±25122	.11±.00
1E	70:30	C	10,845±920	222,231±71441	.13±.01
1F	80:20	C	8,117±381	254,575±14854	.06±.00
2A	50:50	GL/N	11,753±413	249,539±37303	.05±.01
2B	50:50	GT	15,155±331	181,195±13637	.16±.01
2C	70:30	GT/D/N	15,709±1104	151,007±13007	.17±.00
2D	70:30	GL/N	8,911±697	227,540±40460	.13±.01
2E	80:20	C/GL	17,951±1059	330,839±71139	.13±.01
X1	80:20	N	6,835±956	126,199±12240	.13±.01
X2	80:20	GL/N	10,668±1584	164,817±25477	.14±.01
X3	80:20	N/D	8,962±607	186,000±15568	.17±.01
X4	80:20	GL/N	13,815±1680	202,462±53734	.17±.02

*N = nylon; D = dacron; C = cotton; GL = glass, loose weave; GT = glass, tight weave.
**Weight ratio of 4110 resin (American Cyanamid Co.) to Polylite resin (Reichhold Chemicals, Inc.) employed.

SUGGESTIONS FOR IMPROVEMENT

Although one might consider utilizing a stronger material, the basic change should result in a reduction of the high stress concentration produced by the sharp right-angle bend (i.e., the fracture site).

Reduction in stress at the radial edges could be provided by a larger radius, as shown in Figure 6, *left*, but this would change the resistance to both dorsiflexion and plantar flexion. However, failure occurs by fatigue, which is primarily a tensile phenomenon (plantar flexion). Therefore, when an orthosis is required to resist only plantar flexion (high tensile forces), and need not necessarily rigidly counteract compression forces, an orthosis of the type shown in Figure 6, *right*, would suffice. Here a webbing strap provides the resistance to tension during plantar flexion but folds or collapses during compression, thus preventing fatigue failure.

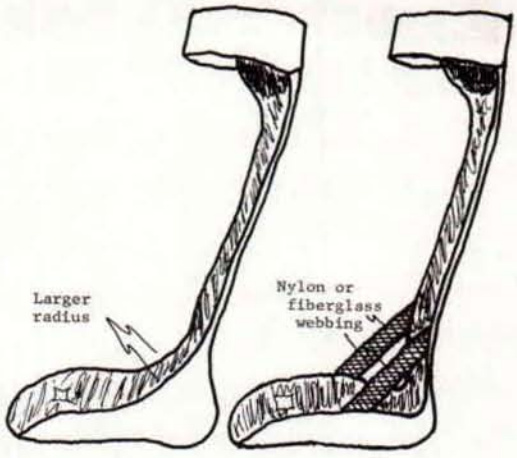

Fig. 6. Two methods of reducing the high tensile stress concentration at the AFO right-angled bend.